An overview of aircraft observations from the Pacific Dust Experiment campaign

Greg Roberts, J. Stith, V. Ramanathan, W. Cooper, P. Demott, G. Carmichael, C. Hatch, B. Adhikary, C. Twohy, D. Rogers, et al.

An overview of aircraft observations from the Pacific Dust Experiment campaign

J. L. Stith,[1] V. Ramanathan,[2] W. A. Cooper,[1] G. C. Roberts,[3] P. J. DeMott,[4] G. Carmichael,[5] C. D. Hatch,[5,6] B. Adhikary,[5] C. H. Twohy,[7] D. C. Rogers,[1] D. Baumgardner,[8] A. J. Prenni,[4] T. Campos,[1,9] RuShan Gao,[10] J. Anderson,[11] and Y. Feng[2]

Received 31 July 2008; revised 18 November 2008; accepted 16 December 2008; published 7 March 2009.

[1] Fourteen research flights were conducted in the Pacific Dust Experiment (PACDEX) during April and May 2007 to sample pollution and dust outbreaks from east Asia as they traveled across the northern Pacific Ocean into North America and interacted with maritime storms. Significant concentrations of black carbon (BC, consisting of soot and other light-absorbing particles measured with a soot photometer 2 instrument) and dust were observed both in the west and east Pacific Ocean from Asian plumes of dust and pollution. BC particles were observed through much of the troposphere, but the major finding is that the percentage of these particles compared with the total number of accumulation mode particles increased significantly (by a factor of 2–4) with increasing altitude, with peak values occurring between 5 and 10 km. Dust plumes had only a small impact on total cloud condensation nuclei at the sampling supersaturations but did exhibit high concentrations of ice nuclei (IN). IN concentrations in dust plumes exceeded typical tropospheric values by 4–20 times and were similar to previous studies in the Saharan aerosol layer when differences in the number concentrations of dust are accounted for. Enhanced IN concentrations were found in the upper troposphere off the coast of North America, providing a first direct validation of the transport of high-IN-containing dust layers near the tropopause entering the North American continent from distant sources. A source-specific chemical transport model was used to predict dust and other aerosols during PACDEX. The model was able to predict several features of the in situ observations, including the general altitudes where BC was found and a peak in the ratio of BC to sulfate between 5 and 10 km.

Citation: Stith, J. L., et al. (2009), An overview of aircraft observations from the Pacific Dust Experiment campaign, *J. Geophys. Res.*, *114*, D05207, doi:10.1029/2008JD010924.

[1]Earth Observing Laboratory, National Center for Atmospheric Research, Boulder, Colorado, USA.
[2]Center for Clouds, Chemistry and Climate, Scripps Institute of Oceanography, La Jolla, California, USA.
[3]Climate, Atmospheric Science and Physical Oceanography, Scripps Institution of Oceanography, University of California, San Diego, La Jolla, California, USA.
[4]Department of Atmospheric Science, Colorado State University, Fort Collins, Colorado, USA.
[5]Center for Global and Regional Environmental Research, University of Iowa, Iowa City, Iowa, USA.
[6]Now at Department of Chemistry, Hendrix College, Conway, Arkansas, USA.
[7]College of Oceanic and Atmospheric Sciences, Oregon State University, Corvallis, Oregon, USA.
[8]Centro de Ciencias de la Atmósfera, Universidad Nacional Autónoma de México, Mexico City, Mexico.
[9]Earth and Sun Systems Laboratory, National Center for Atmospheric Research, Boulder, Colorado, USA.
[10]Chemical Sciences Division, NOAA Earth System Research Laboratory, Boulder, Colorado, USA.
[11]Mechanical and Aerospace Engineering, Arizona State University, Tempe, Arizona, USA.

0148-0227/09/2008JD010924

1. Introduction

[2] Asia is one of the most significant sources of aerosol particles on our planet. These particles have been studied extensively by several recent field projects, such as INDOEX for south Asian pollution plumes [*Ramanathan et al.*, 2001], ACE-Asia [e.g., *Seinfeld et al.*, 2004; *Huebert et al.*, 2003] and TRACE-P [*Jacob et al.*, 2003] for east Asian plumes to better understand their direct radiative impacts on climate and to characterize the south and east Asian chemical outflows and their evolution. However, the effects of dust and pollution (including biomass burning) particles from east Asia on clouds and precipitation are not well known, partly because measurements and observations of the interactions of these emissions with clouds are relatively few. Recently, *Zhang et al.* [2007] attempted to link satellite-observed intensifications of Pacific storm tracks to Asian pollution using a cloud-resolving weather research and forecast model (CR-WRF) by comparing simulations in more polluted conditions with simulations under cleaner conditions. A major limitation for these types of modeling studies is inadequate knowledge of

the activation spectra and spatial variability of cloud active nuclei (i.e., cloud condensation nuclei, CCN, or ice nuclei, IN) to use in the model domain. This problem is especially severe when an area the size of the northern Pacific Ocean is considered, which is necessary for understanding changes on scales important for simulating storm tracks or for climate studies.

[3] Outbreaks of natural dust from Asia are episodic in nature. They are common springtime features that also occur to a lesser extent during the rest of the year, especially for fine (<2.5 μm) dust particles that are thought to affect North America [*VanCuren and Cahill*, 2002]. They produce a significant contribution to the tropospheric aerosol over the western United States [e.g., *Jaffe et al.*, 2005; *Hadley et al.*, 2007]. These dust particles may interact with gaseous pollutants such as SO_2 or other aerosols during their transit, for example by collecting soot or sea salt or by gas to particle conversion. In a dust storm that passed over the Mediterranean Sea, *Levin et al.* [2005] found that some 35% of the coarse particles up to about 1 km in height were internal mixtures of mineral dust and sea salt. When they included these as giant CCN in model simulations of precipitation development they found enhanced development of the warm rain process in continental clouds, but few effects in maritime clouds. *Mahowald and Kiehl* [2003] examined 16 years of observations of mineral aerosols and clouds in the North Atlantic. Their results were consistent with mineral aerosols suppressing precipitation in thin low clouds and changing cloud amounts in ice phase clouds, but they could not demonstrate a causal connection between dust and cloud processes. Recently *Twohy et al.* [2009] have established that Saharan Dust particles commonly act as CCN in the eastern North Atlantic.

[4] Some natural minerals are excellent IN [e.g., *Rogers and Yau*, 1989] and recent studies have confirmed direct connections between airborne dusts, ice nuclei and cold clouds [e.g., *Sassen*, 2002; *Sassen et al.*, 2003; *DeMott et al.*, 2003, and references therein]. *Richardson et al.* [2007] recently provided observations that suggest a link between observed IN in North America and Asian dust sources. The complex way in which dust might affect cloud structure and precipitation is also illustrated by the recent modeling study by *van den Heever et al.* [2006].

[5] In order to understand or simulate the possible effects of Asian emissions on Pacific storms we need to better characterize the sources of both CCN and IN for these storms and the likely contribution that Asian sources make to the observed levels of cloud-active aerosols that are ingested in Pacific storm clouds. Furthermore, observations of changes in the microstructure of clouds caused by these particles are also necessary to validate model simulations or to determine physically the pathways that Asian particles might influence Pacific storms (e.g., via liquid or ice phase mechanisms).

[6] Large Asian dust events have been tracked across the Pacific by satellite [e.g., *Husar et al.*, 2001; *Yu et al.*, 2008], and offer an ideal natural tracer for following the intercontinental transport and transformation of aerosols during their transit. Because much of the cross-Pacific transport is thought to occur at high altitudes [e.g., *Stohl et al.*, 2002, and references therein], measurements of the Asian emissions through the depth of the troposphere and in storms are needed, and these have not previously been available to studies such as ACE-Asia. Because some dust events or portions of the dust plume often mix with pollution, including CCN and CCN precursors, changes due to aerosol chemistry (e.g., the production of CCN by gas to particle conversion) can also be observed. When these plumes of dust or pollution encounter cloud forming conditions during their transit across the ocean, measurements of clouds that contain these cloud active aerosols provide the opportunity to observe possible effects on the cloud microstructure.

[7] The Pacific Dust Experiment (PACDEX) was designed to follow east Asian emissions, especially dust outbreaks, across the northern Pacific Ocean with a long-range research aircraft capable of reaching altitudes covering most of the troposphere and lower stratosphere where clouds associated with northern Pacific storms are found. While major dust outbreaks are readily detected by satellite, smaller dust events are common, especially during the springtime. The ubiquity of dust transport from Asia suggests that these events are likely to be common in the Pacific storm region [*Zhu et al.*, 2007].

[8] In this article we provide an overview of the PACDEX program by describing the major instruments that were employed and the flights that were accomplished during the campaign. We also provide some highlights from the measurements to illustrate some of the early results from the project. Some of the questions that we hope to address from the PACDEX program include the following.

[9] 1. Is Asian dust a significant source of IN to the northern Pacific in the springtime? Do these dust IN survive long enough to impact North America? In this article we provide examples of encounters with dust plumes where both the dust concentration and the IN were measured to illustrate the levels of IN associated with dust events at various Pacific locations and we compare these results with similar observations in the Saharan aerosol layer (SAL) in the Atlantic Ocean.

[10] 2. Can numerical models predict the locations of enhanced dust and IN and therefore the locations where Asian dust might affect cloud microphysics? Here we compare model predictions of dust plume locations with in situ encounters where enhanced IN and dust were observed.

[11] 3. How do the vertical distributions of cloud-active nuclei and soot (and other light absorbing aerosols, which we refer to as black carbon, BC) compare between the western and eastern Pacific? What is the role of clouds and storms in producing observed differences? In this article we present aerosol measurements made during several vertical profiles in the western and eastern Pacific. Early results on the scavenging of BC particles in PACDEX storms are provided by *Baumgardner et al.* [2008].

[12] 4. What are the effects of Asian dust and emissions of cloud active nuclei and soot on northern Pacific maritime storms? In this article we provide examples of the early results from sampling storms in the western Pacific.

[13] The National Science Foundation (NSF)/National Center for Atmospheric Research (NCAR) G-V (also referred to as High-Performance Instrumented Airborne Platform for Environmental Research, HIAPER [*Laursen et al.*, 2006]) was used as the research aircraft. It carried instruments to measure cloud active nuclei, cloud microphysics,

Table 1. Summary of Major PACDEX Instruments[a]

Parameter	Instrument
Black carbon (light-absorbing carbon)	Soot photometer 2 (SP-2)
Individual particle samples	Streaker-sampler and microimpactor
Cloud condensation nuclei	Streamwise thermal gradient chamber
Aerosol particle concentrations between 0.1 and 1 μm	UHSAS optical particle counter
Ice nuclei	Continuous-flow diffusion chamber
Cloud droplet size distribution	Cloud Droplet Probe
Ice and precipitation particle size distributions	Small Ice Detector (SID-2H), in-house modified PMS OAP-2DC
Carbon monoxide	Vacuum UV absorption instrument
Ozone	UV absorption photometer
Spectral irradiances of 300–2200 nm	HIAPER Airborne Radiation Package

[a]See the text for instrument details. Abbreviations are as follows: HIAPER, High-Performance Instrumented Airborne Platform for Environmental Research; PACDEX, Pacific Dust Experiment; UHSAS, Ultra-High Sensitivity Aerosol Spectrometer.

selected aerosol parameters, trace gases, and meteorological parameters.

2. Instrumentation and Methodology

[14] The NSF/NCAR G-V, with its range capabilities of over 8000 km and ceiling of over 15 km, is ideally suited to sample dust events. It is capable of following their progress during advection across horizontal scales large enough to cover much of the Pacific and vertical scales covering most of the midlatitude troposphere where extratropical cyclonic storms are found. Flight plans were designed to utilize this capacity. Flights were planned by reference to meteorological forecasts, satellite products, and chemical transport models of the dust advection for specific dust outbreaks.

2.1. Pacific Dust Experiment (PACDEX) Instrumentation Overview

[15] The NSF/NCAR G-V carries a set of standard instrumentation for measurement of location, temperature, and pressure. An inertial navigation system coupled with a radome gust sensor is used to derive three-component wind and turbulence parameters. Chilled mirror humidity sensors were used for measurement of water vapor in PACDEX. Complete details on each of these standard instruments (range, resolution, accuracy, response time) are provided in http://www.hiaper.ucar.edu/handbook. The PACDEX-specific instruments are listed in Table 1 and described below.

[16] Inlets for bringing air to instruments inside the aircraft cabin during PACDEX were based on the HIAPER Modular Inlets (HIMIL). They were configured for sampling trace gases and aerosol particles. HIMIL is a forward-facing flow-through inlet with a diffusing nozzle upstream and converging nozzle downstream. In PACDEX four such inlets were used. They have calculated particle passing efficiencies of approximately 94 to 110% for particles 1 μm diameter and smaller, over the range of typical G-V sampling altitudes (sea level to 12 km) and airspeeds (120–260 m s^{-1}). (This efficiency does not include downstream tubing that feeds the instruments.) At typical research speeds there should be $\sim$15° to 20°C compressional heating of the air, which is likely to evaporate some volatile components of the aerosol. More information on the HIMIL inlets and the efficiency calculation can be found at http://www.eol.ucar.edu. A Counterflow Virtual Impactor (CVI [*Noone et al.*, 1988; *Twohy et al.*, 1997]) inlet was also flown during PACDEX, and used for measurements of condensed water content (above the CVI threshold size of about 5 μm aerodynamic diameter) and to provide an aerosol sample stream of cloud particle residual for subsequent sampling described below.

[17] Particles containing BC were sampled by a Droplet Measurement Technologies (DMT) single particle soot photometer (SP-2). The technique is described by *Schwarz et al.* [2006]. The SP-2 measures BC mass by laser induced incandescence and particle size by light scattering in the range of 0.08 to 0.3 μm for BC mass equivalent diameter and 0.1 to 0.6 μm optical diameter (BC particles greater than about 0.3 μm saturate the incandescence detector and can be counted but not sized). The estimated uncertainty in BC mass derived from the SP-2 is ±35%. The SP-2 sampled from a HIMIL inlet most of the time during PACDEX, except during some periods in-cloud when its sampling was switched to the CVI. Below we refer to the soot photometer measurements as BC, although strictly speaking the particles do not have to be entirely black to be detected (i.e., both brown and black carbon particles are sampled). This distinction is important because the east Asian outflow contains significant number of brown carbon particles [e.g., *Alexander et al.*, 2008].

[18] Two programmable streaker-samplers (PIXE International) were set up as filter samplers for scanning electron microscope analysis and two three-stage microimpactors (California Measurements, Inc.) were used to collect aerosol by impaction onto 3 mm grids for transmission electron microscope analysis. The 50% cut sizes for the microimpactor were 2.0, 0.3 and 0.05 μm. One set of samplers sampled ambient air through a HIMIL inlet and the other set sampled though the CVI.

[19] Fast-response CCN measurements at two supersaturations (Sc) were made with a dual-column continuous-flow streamwise thermal gradient CCN chamber manufactured by DMT and based on a design described by *Roberts and Nenes* [2005]. The dual column instrument measured CCN concentrations at two supersaturations simultaneously at 1 Hz. To maintain constant Sc while the aircraft changed altitude, the internal pressure of each CCN column was maintained at 400 hPa via a constant pressure controller—allowing profiles of CCN up to 6000 m above sea level. At altitudes higher than 400 hPa, only data from level legs are used and the supersaturation is recalculated based on laboratory calibrations. Data are reported per cm^3 at ambient conditions, for comparison with droplet concentrations.

[20] Cloud droplets and large aerosols were measured with a wing mounted Cloud Droplet Probe (CDP, made by

DMT). The CDP is an open path single particle forward-scattering instrument, designed for airborne use and covering the size range 2–50 μm diameter at speeds up to 250 m s^{-1}. The CDP was designed for cloud measurements but it measures light scattering from any particle larger than about 2 μm, although nonspherical particles will be undersized. Large aerosol particles are measured but the small sample area of the CDP limits the sampling statistics for these particles unless averages are taken over several tens of kilometers.

[21] Particle concentrations and sizes between 0.1 and 1.0 μm were measured in situ by a wing-mounted Ultra-High Sensitivity Aerosol Spectrometer (UHSAS, manufactured by DMT), an optical particle counter with 100 channels covering the range nominally from 0.075 to 1.0 μm. (Only sizes above 0.1 μm are used here because of noise problems in the lower channels). The UHSAS is a new instrument that shares a similar geometry with the PCASP (also by DMT) which has been used in airborne applications for many years. The UHSAS incorporates a new laser and signal processing system and better flow control regulation than the PCASP. These improvements allow for operation at higher altitudes on the G-V. For PACDEX the UHSAS was operated without its real-time gain stage matching feature, which is not expected to significantly affect the integrated particle concentrations presented here, but it produced some irregularities in the differential size distribution, which can be corrected by combining channels in regions of gain stage overlap.

[22] We use the UHSAS number concentration for sizes between 0.5 and 1.0 μm as a surrogate for dust (except in the lower marine troposphere, where sea salt is likely to be present) and refer to them as large aerosols in this article. A larger lower threshold might be better at avoiding interference with pollution particles, but this size range is chosen to be most comparable to the IN measurements. UHSAS 0.1 to 1.0 micron particles are presented at 1 Hz, while UHSAS 0.5 to 1.0 μm time series data were averaged using a 20 s running mean applied to 1 Hz data to smooth irregularities caused by low counts in the 1 Hz data. In PACDEX, during periods of enhanced concentrations in the 0.5 to 1.0 μm size range the CDP often indicated the presence of supermicron particles outside of clouds.

[23] Although most of the mass of Asian dust is expected to be in sizes above 1 μm, the size range above about 0.5 μm should be elevated in number concentration during significant dust events. For example, for emissions sampled during the ACE-Asia project, *Kline et al.* [2004] have shown that concentrations of calcium (an indicator of dust) in airborne samples were highest in the coarse particle mass mode above 1 μm, but also had significant mass concentrations in the range of 0.5 to 1.0 μm. For mineral dust particles coming from North Africa, *Maring et al.* [2003] suggested that dust particles were essentially the only particles with diameters >0.6 μm present in the free troposphere in the Canary Islands and used measurements of aerosol size distributions for diameters >0.6 as direct measurements of dust particles at that site. During PACDEX samples for chemical analysis and electron microscopy were taken in many of the regions where this size range exhibited enhanced concentrations and are currently undergoing analysis. The scanning electron microscope observations that have been examined to date confirm the presence of dust in these regions; however, there are also significant numbers of BC and sea salt particles in some of these samples with the ratio of dust to these others varying from sample to sample.

[24] Elevated IN number concentrations are expected to be associated with mineral layers on the basis of a large body of literature dating back a half century [*Pruppacher and Klett*, 1997]. Recent observations within the SAL [*DeMott et al.*, 2003] confirm the presence of large numbers of IN in the SAL (after transport to the Florida region), which we compare with PACDEX measurements of IN in Asian dust in the Pacific, below.

[25] A continuous-flow (ice-thermal) diffusion chamber (CFDC), was used to measure IN. The CFDC is a device for processing populations of aerosol particles at cloud environmental conditions in order to promote ice formation by those particles capable of acting as ice nuclei [*Rogers*, 1988; *Rogers et al.*, 2001]. The technique is most sensitive to deposition and condensation/immersion freezing nucleation due to limited (~10 s) residence times, so we note that not all IN are sampled (e.g., some contact nuclei). However, here we retain the IN acronym to refer to the measurements from the CFDC. During PACDEX, the typical conditions in the CFDC for processing aerosols in the lower troposphere were generally a few percent greater than water saturation to favor condensation/immersion freezing. Measurements in the upper troposphere and occasional measurements in the lower troposphere were also made below water saturation, which allows the IN component due to deposition only to be measured. Measurements are also limited at present to aerosol particles smaller than about 1 μm in order to prevent false positive identification of large aerosol particles as nucleated ice crystals. This is accomplished by operating an impactor upstream of the CFDC. The CFDC sampled through a HIMIL inlet, except when in cloud, when sampling was usually switched to the CVI. IN data are reported here as 60 s running mean values. Measured IN concentrations represent values at a specific processing temperature and relative humidity at any time.

[26] A Small Ice Detector, version 2 (SID-2H), was available for the first half of PACDEX. SID-2H is a single particle optical scattering instrument. It has multiple detectors to measure scattering asymmetry, from which small ice particles and small water drops can be discriminated [*Hirst et al.*, 2001].

[27] Precipitation-sized particles were measured with a specially modified PMS OAP-2DC optical array instrument, which used high-speed electronics and a 64-element diode array in order to shadow particles at the sampling speeds of the G-V aircraft. During the first six PACDEX flights, image data are not available, but the sizes could be reconstructed by referencing the maximum number of diodes occluded. For the remainder of the flights image data were available.

[28] Carbon monoxide measurements were made using a vacuum UV absorption method for CO. The precision of the CO instrument is 3 ppbv for a 1 Hz sample rate. Ozone measurements were made with a dual-beam UV-absorption ozone photometer with an overall uncertainty of ±5% and precision of 1.5×10^{10} molecules/cm3 (~1 ppb at 200 hPa) [*Proffitt and McLaughlin*, 1983]. These instruments can detect and measure both concentrations of these gases both in plumes and in the clean ambient air.

Table 2. Summary of PACDEX Missions in 2007[a]

Flight Identifier	Time and Date (UT)	Origin and Destination	Features
RF01	1602–2336, 29 Apr	Colorado–Alaska	Sampling cirrus and marine stratus in varying levels of pollution
RF02	1758–0254, 30 Apr to 1 May	Alaska–Japan	Vertical profiles of pollution in western Pacific
RF03	0235–1039, 2 May	Japan–Japan	Pollution profiles, marine stratus, and cirrus sampling
RF04	0355–1229, 3 May	Japan–Alaska	Mid-Pacific vertical profiles in and out of clouds; high concentrations of large particles observed
RF05	1701–0126, 5–6 May	Alaska–Alaska	Detailed sampling of storm in mid-Pacific
RF06	1656–0045, 6–7 May	Alaska–Colorado	Continued sampling of storm from RF05; sampling of marine stratus in eastern Pacific
RF07	1453–2218, 13 May	Colorado–Hawaii	Large particle encounters in eastern Pacific; vertical profiles in mid-Pacific; occasional cloud encounters
RF08	1907–0236, 14–15 May	Hawaii–Alaska	Detailed sampling of storm between Hawaii and Alaska
RF09	1953–0452, 15–16 May	Alaska–Japan	Large particle sampling and vertical profiles
RF10	0120–1023, 17 May	Japan–Japan	Detailed sampling of storm in western Pacific
RF11	2312–0823, 19–20 May	Japan–Japan	Detailed sampling of storm in western Pacific
RF12	0027–0851, 22 May	Japan–Japan	Detailed sampling of storm in western Pacific; encounter with high-altitude large particles
RF13	0228–1019, 23 May	Japan–Hawaii	Tracking of suspected dust plume between Japan and Hawaii; midflight vertical profiles through clouds and pollution
RF14	1916–0247, 24–25 May	Hawaii–Colorado	Northbound tracking of suspected dust plume; cirrus and marine stratus sampling; vertical profiles of pollution

[a]PACDEX, Pacific Dust Experiment.

[29] Radiation measurements were made using the HIAPER Airborne Radiation Package (HARP). It includes the down and up welling spectral irradiances in the wavelength range from 300 to 2200 nm at various spectral resolutions using UV visible and near-infrared spectrometers and actinic flux instruments. This instrument is suitable for determining layer properties, such as reflectance, transmittance and absorptance and for deriving broadband solar irradiances. The instrument is derived from a predecessor described by *Pilewskie et al.* [2003] and has similar characteristics.

2.2. Flight Procedures and the Forecast Dust Environment During PACDEX

[30] Several source-specific chemical transport models were used to guide the research flights. For example, forecasts of dust concentrations made with the Sulfur Transport and Deposition Model (STEM [*Carmichael et al.*, 2003]) chemical modeling system were used to plan flights to intersect forecast dust plumes and clouds. Updated model and satellite products were also relayed to the aircraft in flight via a satellite communication relay. This allowed for real-time modification of the flight plans to intersect areas of interest.

[31] When the opportunity arose, a series of semi-Lagrangian type flights were flown to sample dust plumes as they traveled across the Pacific. Fourteen research flights occurred throughout two trips across the Pacific, during April and May 2007. Flights from Colorado originated from Broomfield, Colorado; flights from Alaska originated from Anchorage, Alaska; flights from Japan originated from Yokota Air Force Base; and flights from Hawaii originated from Honolulu, Hawaii. A listing of the flights and their purpose is provided in Table 2. Typical flight profiles included descents and ascents in regions of interest (e.g., areas where dust was suspected) to locate plume features and horizontal passes through regions of interest. The descents and ascents are used to construct vertical profiles of measured parameters, although these profiles also include some horizontal variations. All flights, including ferries between locations, included sampling maneuvers (descents, legs through regions of interest, etc.).

[32] Airborne and supporting data are archived at the National Center for Atmospheric Research, Earth Observing Laboratory.

3. Highlights of Aircraft Observations From the PACDEX Campaign

3.1. Ice Nuclei and Cloud Condensation Nuclei in a Mid-Pacific Dust Encounter

[33] During the period 22 to 25 May 2007, we utilized guidance from STEM to follow a dust outbreak from near Japan to the eastern Pacific with three flights: RF12, RF13, and RF14 (Table 2). Dust was encountered in each of these flights. The formation of the dust event, the changes in the distribution of dust during transit, and the sources of sampled air during these flights is clearly illustrated in the STEM forecasts and calculated back trajectories (Figure 1). An example of the PACDEX results from these flights is provided by a dust encounter during a vertical profile that was conducted between 0746 and 0803 UT near 29°N, 173°W (Figure 1, middle) on 23 May. The STEM forecast on that date clearly shows a narrow band of dust had been predicted near the location where the profile was made. Some of the results from the aerosol measurements made during this profile are given in Figure 2. For the data collected in the upper part of the vertical profile (above the arrow in Figure 2), the CFDC was operated below water saturation and in the lower part of the profile it was operated above water saturation. In the water supersaturated region, IN number concentrations up to nearly 40 per liter (at 102% relative humidity with respect to water (RHw) and −32°C) were found in the dust plume, exceeding the range of typical tropospheric values [*Möhler et al.*, 2007] by 4 to 20 times at the CFDC processing conditions.

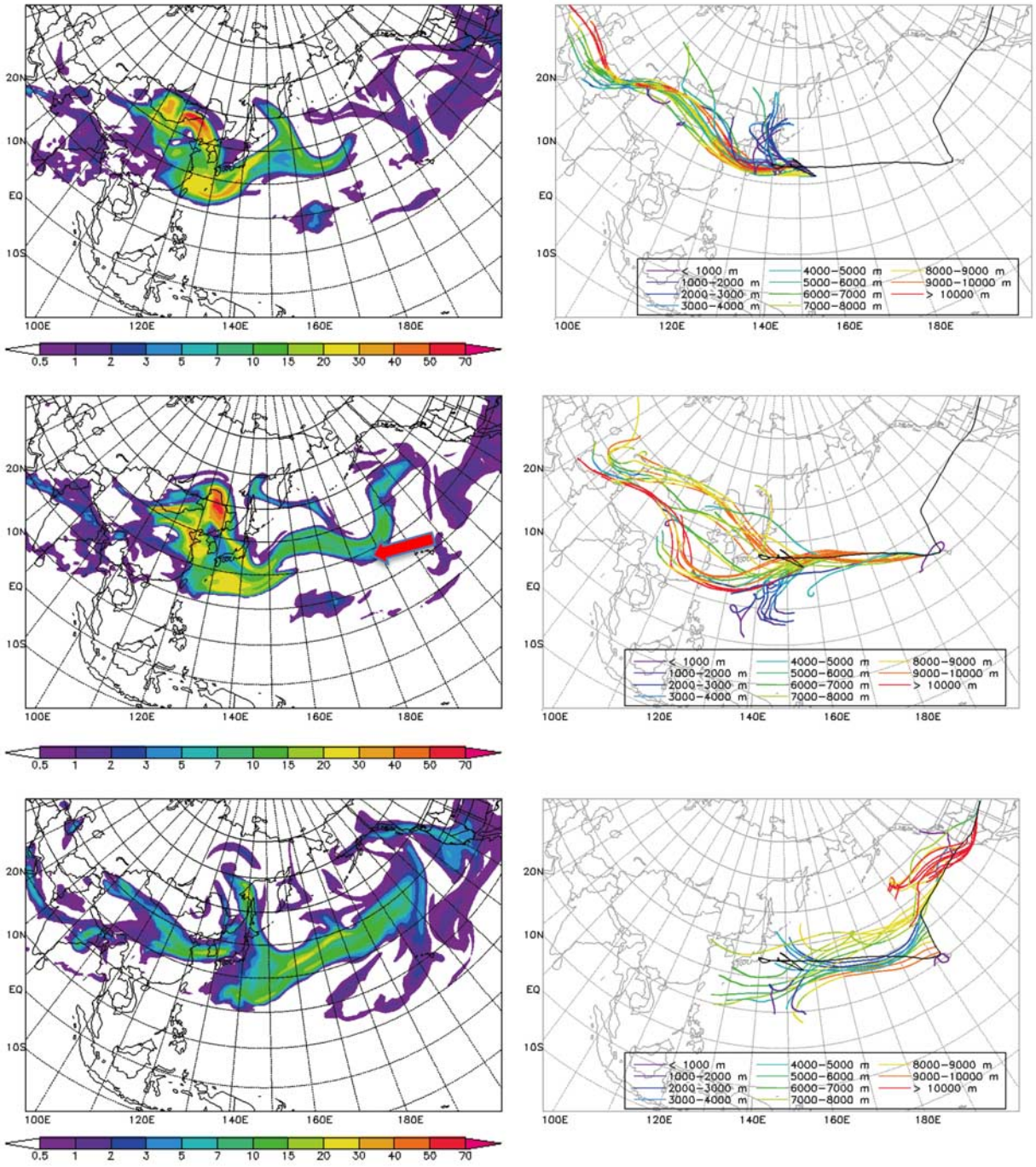

Figure 1. Sulfur Transport and Deposition Model (STEM) dust forecasts for 22–25 May 2007 at 8.4 km at 0000 UTC on (top) 22 May (RF12), (middle) 23 May (RF13), and (bottom) 25 May (RF14). Calculated backward trajectories (over 4 days) along the flight tracks are shown on the right side. The approximate location of the dust encounter shown in Figure 2 is indicated by the red arrow in the forecast for RF13. The track of the aircraft during these flights is given by the black line in the right-hand panels.

[34] The lower numbers of IN compared to large aerosols in the layer above about 8 km in Figure 2 are clearly related to the transition of processing RHw from below water saturation above 8 km to water supersaturated conditions during descent to lower altitudes. This behavior reflects the lower number of active IN in the deposition ice nucleation regime, a factor previously noted in general for IN sampled in the midlatitude upper troposphere [*DeMott et al.*, 1998] and Arctic lower troposphere [*Prenni et al.*, 2007]. Figure 2 demonstrates this ice nucleation characteristic for the first time for aerosols within a long-range transported dust plume. This observation also confirms in the atmosphere a behavior of natural dust particle ice nucleation previously noted only in laboratory studies. Namely, that the strongest

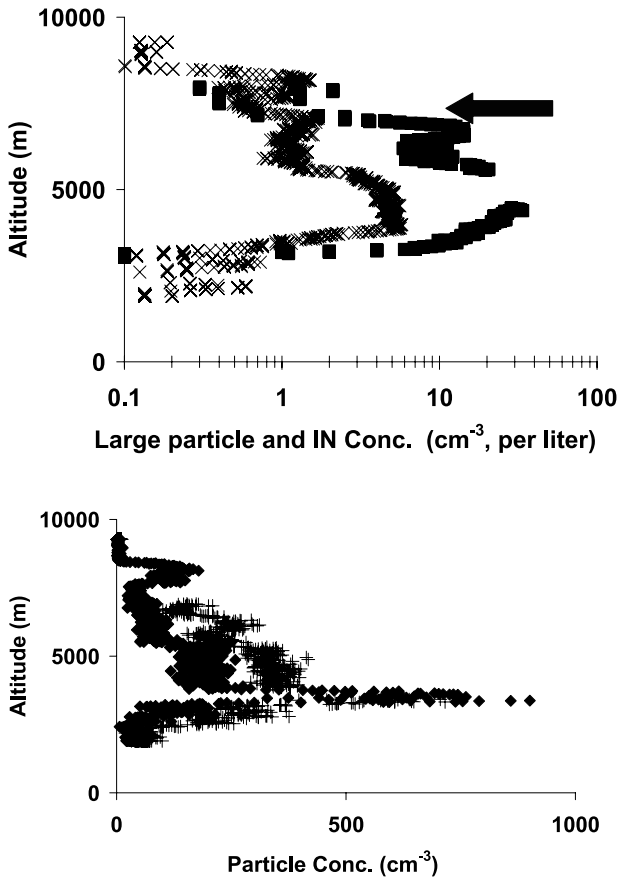

Figure 2. The results of a vertical profile made through a forecast dust region on 23 May 2007 between Japan and Hawaii in the region indicated by the arrow in Figure 1. (top) Concentrations of 0.5–1.0 μm particles (crosses) and ice nuclei (IN) at −32°C (solid squares). The continuous-flow diffusion chamber (CFDC) was processing at or above water saturation at altitudes below the level of the arrow. (bottom) Concentrations of 0.1–1.0 μm particles (solid diamonds) and cloud condensation nuclei (CCN) at 0.45% Sc (pluses).

ice activation of Asian desert dust particles is found in most cases to occur only as water saturation conditions are approached from lower RHw at temperatures warmer than the homogeneous freezing temperature of pure water [*Field et al.*, 2006]. IN number concentrations have previously been observed to trend with the number concentrations of larger aerosols in past atmospheric sampling at surface sites [*Georgii and Kleinjung*, 1967; *DeMott et al.*, 2003; *Richardson et al.*, 2007].

[35] The observed IN number concentrations of 40 per liter in the middle of the Asian dust layer in Figure 2 occur in association with large particle number concentrations of about 5 cm^{-3}. (The highest large particle concentrations found in dust conditions during PACDEX were up to 50 cm^{-3}, but IN measurements were not available during these periods). IN concentrations of 300 per liter (at 87% RHw at −36°C) were found in the SAL case, as reanalyzed by P. J. DeMott et al. (Correction to "African dust aerosols as atmospheric ice nuclei," submitted to *Geophysical Research Letters*, 2009), in association with large particle concentrations of 20 cm^{-3}. Thus, relative to the large particle (dust) number concentrations, these measurements in Asian and Saharan dust plumes indicate high IN number concentrations that differ only by about a factor of 2, when changes in large particle concentrations are accounted for. It is not known to what extent this modest difference is due to the difference in the processing conditions or in differences in the basic ice nucleation properties of dusts from the two sources. Nevertheless, the general correspondence of IN numbers from the two sources at proximal processing conditions is remarkable.

[36] CCN (at 0.45% Sc) correlated with the concentrations of 0.1 to 1.0 μm particles and displayed a peak of just over 700 cm^{-3} at 3.5 km altitude, below the location of the main IN and dust region. This CCN peak corresponded to a peak in CO, ozone and BC (not shown), which suggests that most CCN were concentrated in a thin layer of pollution. CCN concentrations in the main region of dust were about a factor of two lower. The main region of IN in this profile was in the dust layer, just above a layer of CCN-rich pollution. A layer of dust situated above a sulfate-rich pollution plume was also noted in the ACE-Asia study downwind of the Korean peninsula by *Seinfeld et al.* [2004].

3.2. Dust Ice Nuclei Arriving at North America: A High-Altitude Eastern Pacific Encounter

[37] *VanCuren and Cahill* [2002], on the basis of ground measurements of Asian dust at various elevations in North America, concluded that Asian dust in North America is concentrated in an altitude zone between 500 to 3000 m (MSL). *Richardson et al.* [2007] noted that a global aerosol transport model predicted frequent incursions of dust to much higher altitudes. In accord with this suggestion, we encountered dust near 13 km altitude in the eastern Pacific approaching the west coast of North America on 13 May 2007. Examination of the STEM near the location and time where dust was found (Figure 3, bottom) suggested the presence of dust from an event that began its traverse of the Pacific at 06 UTC on 10 May 2007 (Figure 3, top).

[38] Particle concentrations measured during this encounter are presented in Figure 4. The dust was detected as the aircraft descended from 13.3 to 12.5 km altitude, and transitioned from the stratosphere (chemical) to the troposphere (arrow in Figure 4), based on measurements of ozone changes from about 400 ppbv to 110 ppbv (not shown). Evidently, the tropopause served as a vertical cap to the dust plume. The CDP responded with occasional counts in the presence of the large aerosol (the instrument has a nominal lower cutoff of 2 μm for water droplets), also confirming the presence of dust particles (this response from the CDP was observed in the other PACDEX dust encounters).

[39] IN number concentrations shown in the upper tropospheric dust plume in Figure 4 were collected for CFDC processing of aerosols at 75–83% RHw at −35°C, in the deposition nucleation regime. Higher IN values were correlated with the higher RHw values. For this reason and since, as noted above, most dust particles require RHw close to 100% for strongest activation at this temperature [*Field et al.*, 2006], these measurements should be considered lower bounds for estimates of IN concentrations relevant for

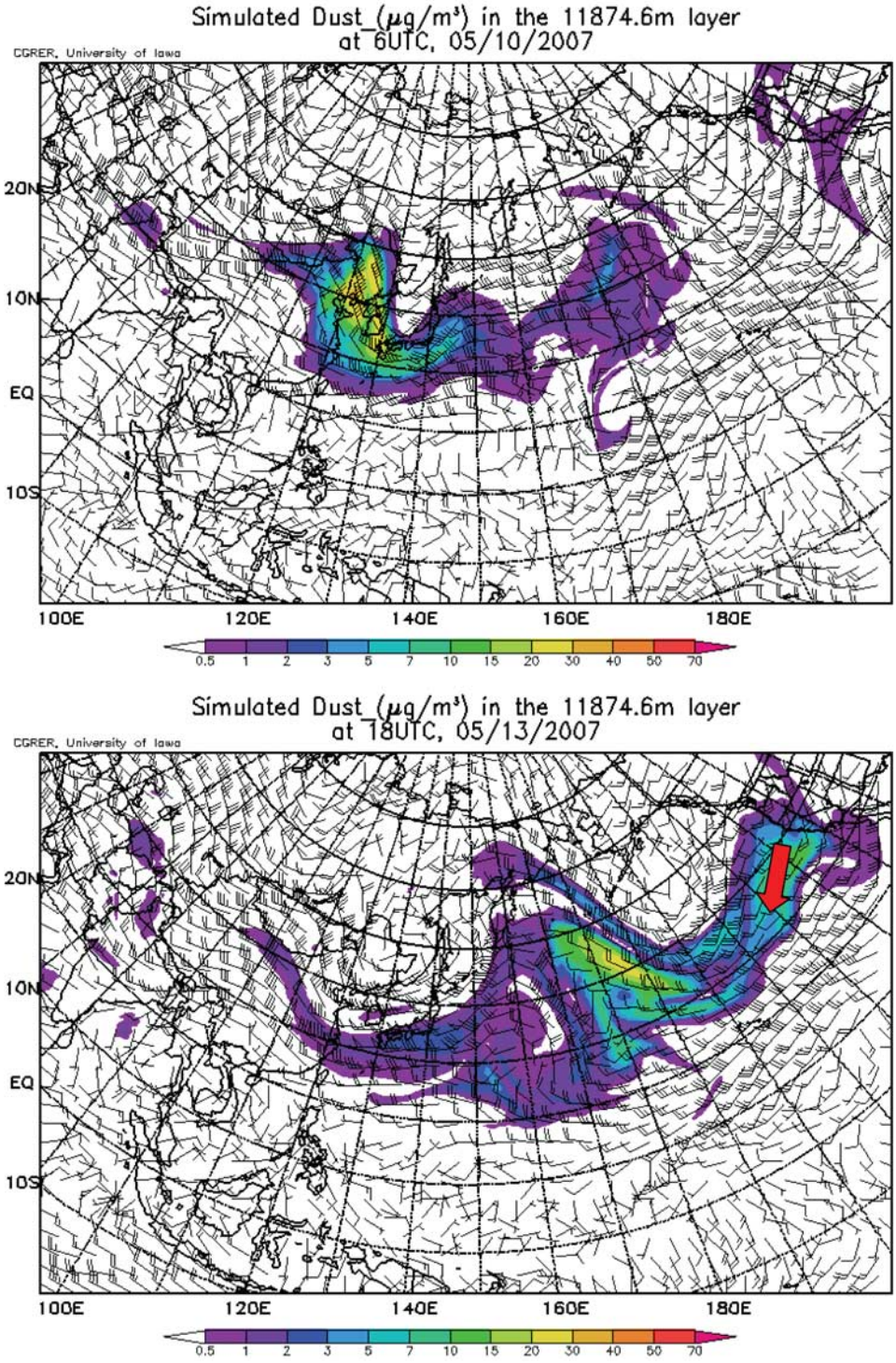

Figure 3. STEM simulations of a dust outbreak between 10 and 13 May 2007. (top) Early stages of the dust event. (bottom) Subsequent transport to the sampling location. The red arrow shows the approximate location where the dust encounter occurred (Figure 4).

mixed-phase and cirrus clouds. Nevertheless, these IN number concentrations up to several per liter are significant for potential impacts on cirrus and precipitating clouds.

[40] Comparing the IN and large particle measurements made below water saturation in Figure 2 (above arrow) from the mid-Pacific, midtropospheric sample, with the upper tropospheric, eastern Pacific sample made below water saturation in Figure 4, suggests that similar concentrations of dust and IN were present in both regions. Comparison of the STEM predicted dust loadings for the two cases (Figures 1

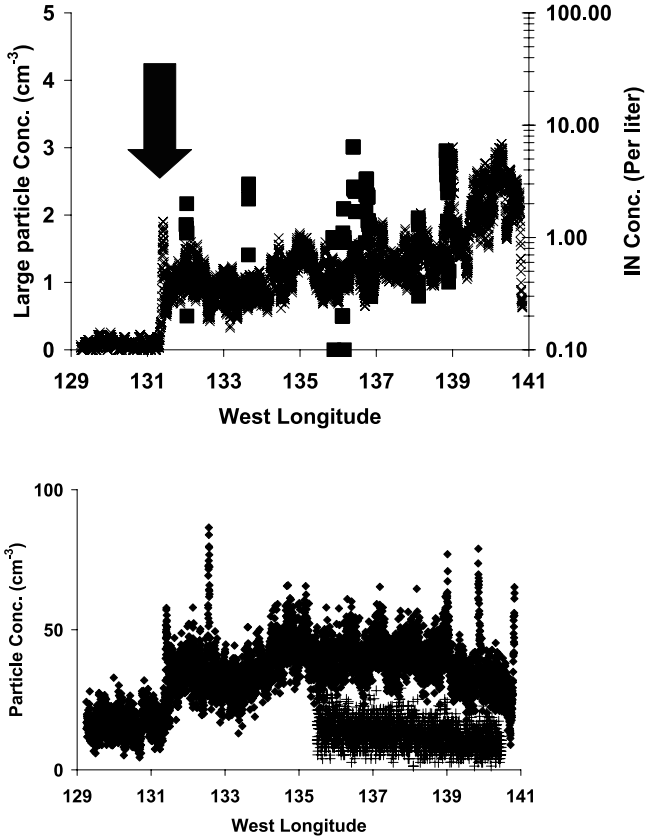

Figure 4. The results of a dust encounter on 13 May 2007 in the eastern Pacific between 13.3 and 12.5 km altitude. (top) Concentrations of 0.5–1.0 μm particles (crosses) and IN at $-32°$ to $-36°$C (solid squares). (bottom) Concentrations of 0.1–1.0 μm particles (solid diamonds) and CCN at 0.45% Sc (plusses). IN data are omitted when unavailable or below 0.1 per liter. The approximate location of the tropopause is indicated by the arrow (troposphere to the right).

and 3) also shows generally similar levels of dust were present in both cases.

3.3. Clear Air Aerosol Profiles in the Eastern and Western Pacific: Comparison of Observed Features With the Sulfur Transport and Deposition Model Predictions

[41] The STEM-predicted mean distributions of dust, sulfate and BC are shown in Figure 5 for the entire set of PACDEX flights. The dominant source regions for dust from the Gobi and Taklimakan deserts, and the anthropogenic sources in eastern Asia are clearly shown. The transpacific transport during this period was aligned along a 35°N axis. A clear demarcation between higher aerosols in the western Pacific and lower aerosols in the eastern Pacific is displayed by the STEM results in Figure 5 and this was generally true for each of the categories of aerosol.

[42] Several in situ vertical profiles were made out of cloud (except for occasional encounters with marine stratus at the bottom of the profiles, which were common) at various locations between Japan and North America (Figure 5a). We divide the profiles that were made into those that occurred in the western and eastern Pacific (west and east of the International Date Line) and display the results for BC to illustrate the comparisons of the PACDEX data with the STEM (Figure 6). Several features are evident from the following results.

[43] 1. The contrast between the higher concentrations in the western Pacific and the lower concentrations in the eastern Pacific is seen in both the model and the in situ observations.

[44] 2. Higher-concentration plumes of BC are evident below about 6 km altitude in both the western and eastern Pacific in both the model and measured profiles. At higher altitudes background levels of BC were of the order of 0.01 μg m^{-3}. (This was also observed outside of plume regions in both locations).

[45] 3. The average concentrations of BC predicted by the STEM model are generally similar to those observed in the vertical profiles at the locations where the sampling occurred. More detailed flight-track-specific comparisons are planned for future studies.

3.4. Abundance of BC Relative to Accumulation Mode Aerosols: Evidence for a Midtropospheric Maximum in the Study Region

[46] Although the general features of the Pacific aerosol we sampled are represented by the horizontal and vertical gradients displayed in Figures 5 and 6, changes in the removal rates or production rates (e.g., by gas to particle conversion) are expected to be different for the different types of aerosol, owing to differences in their sizes and chemical composition. These differences should show up as changes in the relative abundance of particles of different types. To look for evidence of these differences in the observations we examined the ratio of BC number concentrations to accumulation mode aerosol number concentrations (0.1–1.0 μm). The results are displayed in Figures 7b and 7c. The results from the vertical profiles suggest that this ratio increases with altitude, reaching a maximum at about 10 km altitude. For comparison, we examine the ratio of the STEM predictions of BC to sulfates (which are available as a mass ratio) in Figure 7a. STEM predicts that this ratio increases with altitude between 5 to 10 km in the locations that were sampled, and also predicts a general west to east decrease in the ratio (which is less clear in the in situ profiles) and increasing ratios at lower altitudes (which is not evident in the in situ profiles). Thus, both the measurements and predictions suggest a maximum in BC relative to sulfates or accumulation mode aerosol in the mid troposphere between 5 and 10 km, but exhibit less agreement at lower altitudes. These apparent features of Pacific BC aerosols, possibly related to how BC is scavenged by clouds relative to sulfate particles, will be examined further in future articles.

3.5. An Example of the Interaction of Asian Emissions With a Maritime Pacific Storm

[47] One of the objectives of PACDEX was to document the interactions of Asian emissions with Pacific maritime storms. Studies such as *Zhang et al.*'s [2007], which model the effects of storm-ingested aerosols, are not applicable to Pacific storms if Asian aerosols do not actually get ingested into Pacific storms in sufficient numbers to affect the storms. However, there are few studies available that examine actual interactions of Asian aerosols with storms in the Pacific.

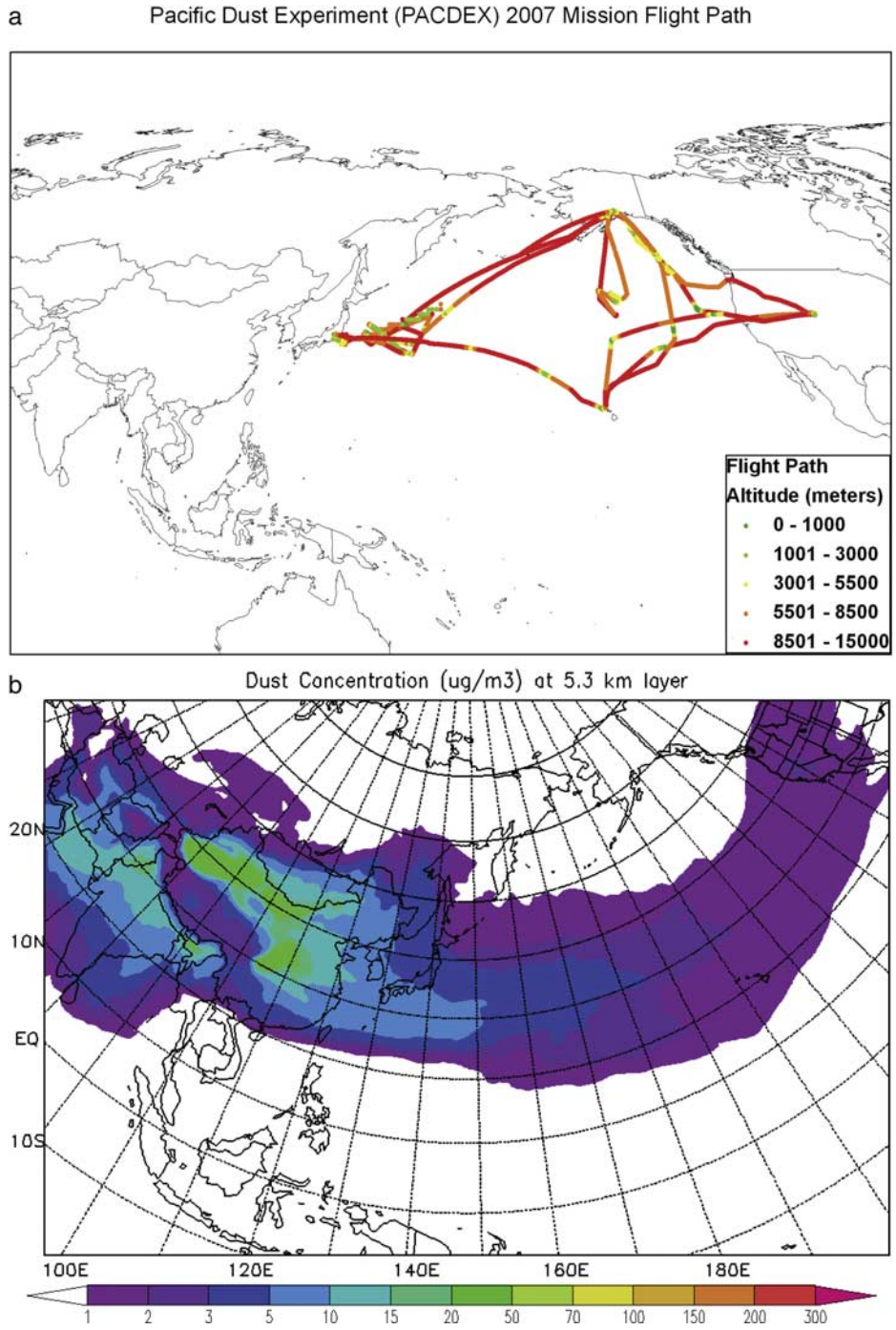

Figure 5. (a) The National Science Foundation/National Center for Atmospheric Research Gulfstream-V research aircraft (G-V) flight tracks during the Pacific Dust Experiment (PACDEX) missions, showing locations of vertical profiles and horizontal transects. (b) Mission-wide STEM calculated averages of mineral dust at the 5.3 km (aboveground level) layer during the PACDEX mission. (c) Same as Figure 5b, except for the concentration of black carbon (BC). (d) Same as Figure 5b, except for the concentration of sulfates.

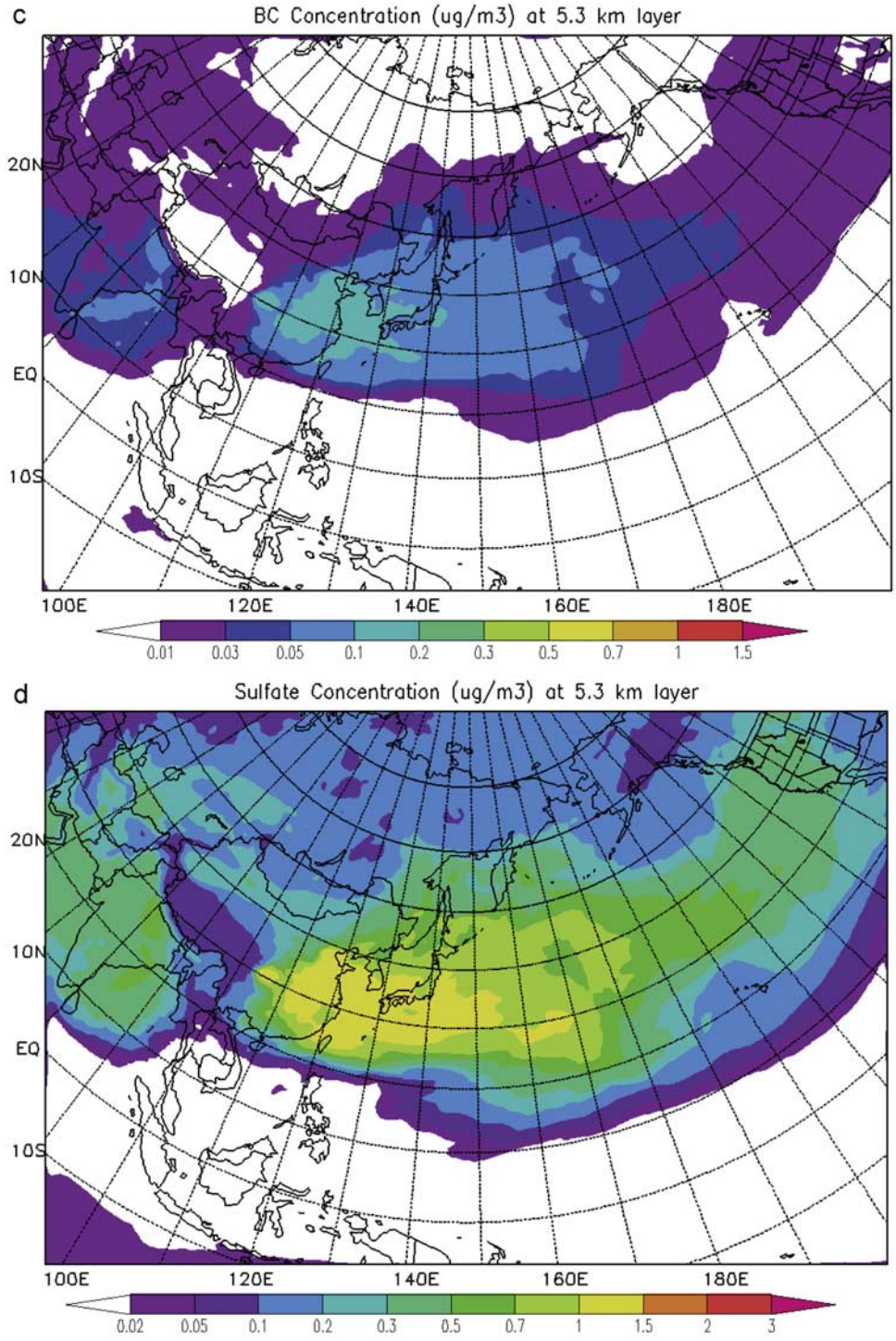

Figure 5. (continued)

These large storms require long sampling legs to observe storm-scale changes in levels of pollution or aerosols. In this section we describe the results from one such leg, where Asian pollution was observed in a storm that is similar to the simulation by Zhang et al.

[48] The pass was made near the freezing level of an extratropical cyclonic maritime storm, just east of Japan, on 20 May 2007 (RF11). The results are presented in Figures 8 and 9. The pass was started just west of the low-level cold front, sampling the storm's cold sector air westbound over a distance of nearly 400 km (Figure 9). Systematic increases in cloud droplet concentration and CCN were observed in cold-sector convective clouds which corresponded to gradually increasing levels of pollution (CO, and BC) along the track toward Japan. The updrafts increased in the mid portion of the pass which likely contributed to activating more CCN, and also may have been a factor in transporting lower polluted air from lower levels to cloud levels. Liquid water concentrations also coincided with the stronger updrafts, suggesting that these clouds were deeper or

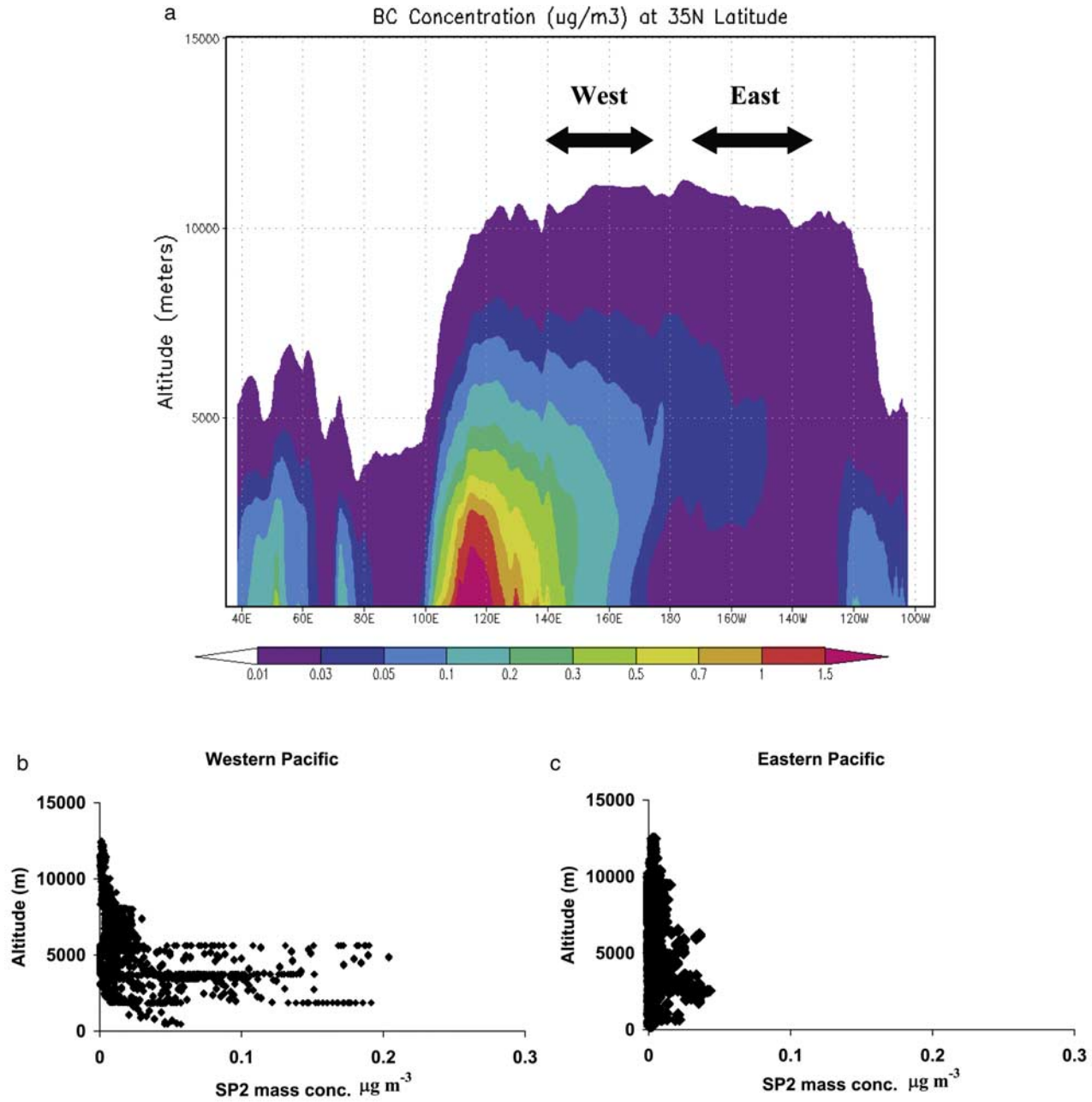

Figure 6. (a) Vertical cross section along 35°N of STEM results for BC average mass concentration during the PACDEX missions. The arrows indicate the longitude locations of vertical profiles of in situ BC presented in Figures 6b and 6c for the western and eastern Pacific, respectively. (b) Composite vertical profiles of in situ BC from the single particle soot photometer (SP-2) instrument taken during RF02, RF03, RF04, and RF13 in the western Pacific. (c) Same as Figure 6b, except for four flights in the eastern Pacific: RF06, RF07, RF13, and RF14.

had less entrainment at the sampling levels. Comparing regions with similar peak updraft strengths on the polluted western side around 0441 UT and on the cleaner eastern side around 0410 UT, we see that the liquid water was higher on the western side (about 0.8 versus 0.4 g m^{-3} on the eastern side); the droplet effective radius was smaller on the western side (7.4 versus 11 μm on the eastern side) and the droplet concentration almost doubled on the western side (about 660 versus 350 cm^{-3} on the eastern side), as shown in Figure 8. This is in line with an effect due to the increasing CCN concentrations.

[49] Although the effects of CCN on the microphysical properties of the clouds sampled in RF11 are evident, the time series shown in Figures 8 and 9 is the only case to date among the several Pacific storms sampled in PACDEX where a clear effect due to pollution-enhanced CCN has been found and only a small horizontal portion of the storm appears to have been affected. Nearer to the main storm frontal region,

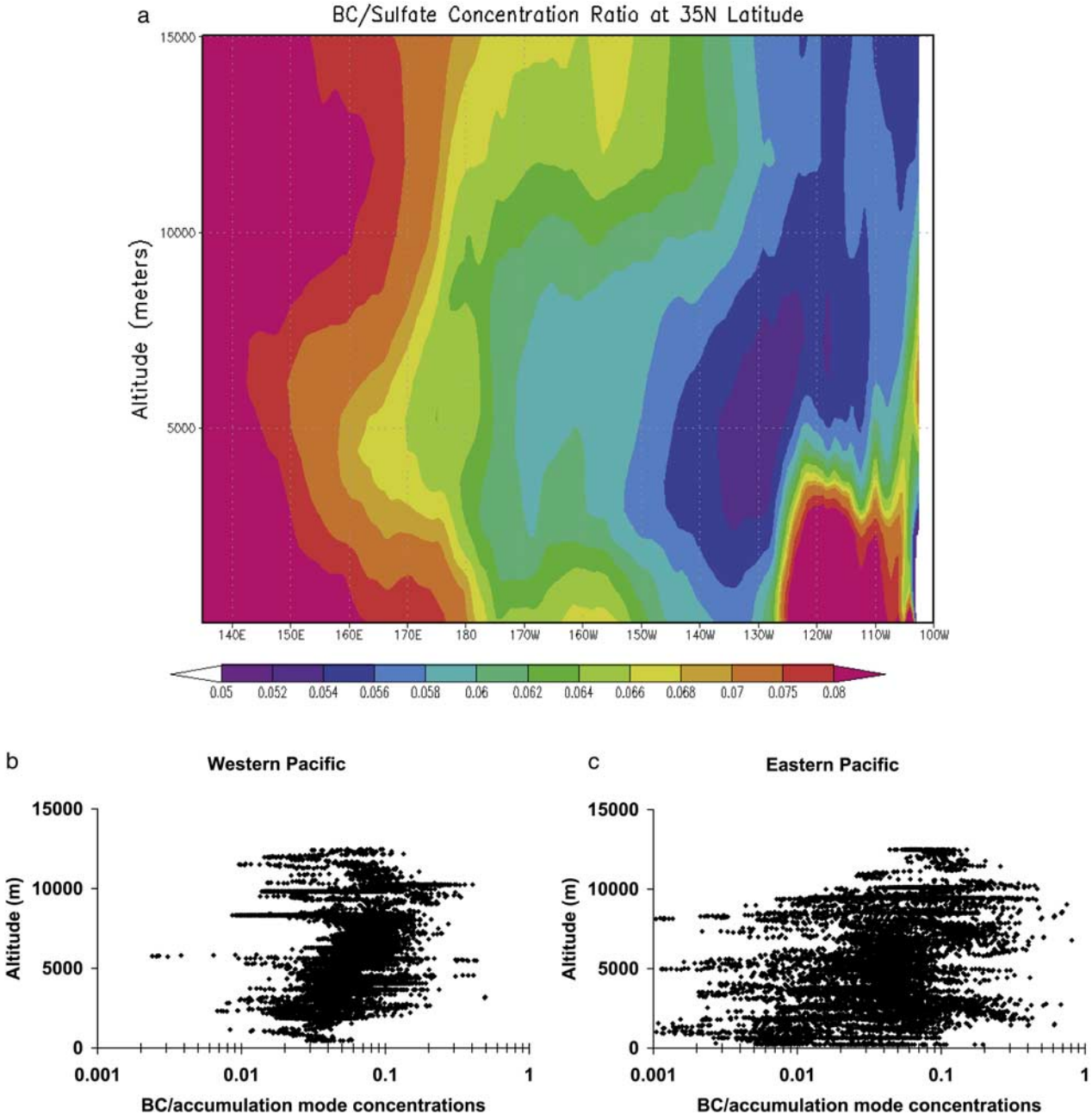

Figure 7. (a) STEM forecast of the ratio of the BC mass concentration to the sulfate mass concentration for the PACDEX flights. (Note the scale change in longitude from Figure 6.) (b) Ratio of the number concentration of BC particles from the SP-2 to the accumulation mode particles (0.1–1.0 μm) from the Ultra-High Sensitivity Aerosol Spectrometer, measured in the western Pacific vertical profiles from RF02, RF03, RF04, and RF13. (c) Same as Figure 7b, except for four flights in the eastern Pacific: RF06, RF07, RF13, and RF14.

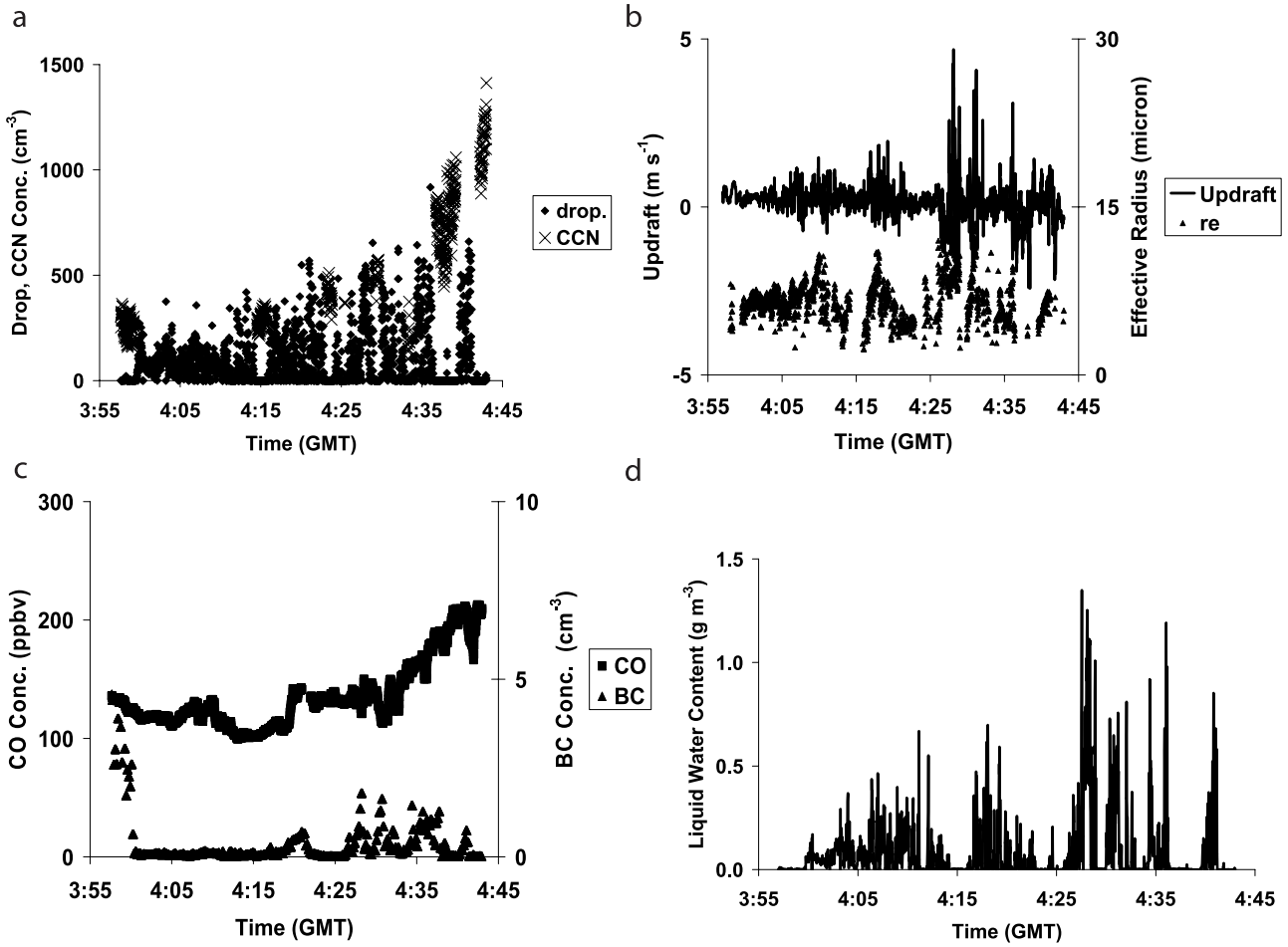

Figure 8. The concentrations of CCN (at 0.12% supersaturation) and (a) droplet concentrations, (b) updraft and effective droplet radius, (c) CO and BC concentrations, and (d) liquid water content for a westbound pass near the freezing level on 20 May 2007, through a storm just east of Japan.

maritime drop concentrations were found (e.g., the left hand side of Figure 8), which are consistent with a non polluted air mass or an air mass where scavenging of CCN has already occurred, rather than the more widespread effects simulated by *Zhang et al.* [2007].

4. Discussion

[50] Areas where Asian dust was found exhibited greatly enhanced concentrations of IN and were remarkably similar to previous IN measurements in the SAL, after differences in the concentrations of dust are taken into account. The observed levels of Asian IN measured below water saturation at high altitude, even on the eastern part of the Pacific (Figure 4), are significant for potential effects on cirrus and on the development of precipitation in North American clouds. At water saturation conditions dust plumes such as the one in Figure 4 would contain substantially greater numbers of IN (roughly an order of magnitude increase, such as the results displayed in Figure 2). Values of similar magnitude have previously been noted during dust transports detected at a mountaintop site in Colorado [*Richardson et al.*, 2007]. That same article made inferences to similar values being commonly present in the upper troposphere during spring based on global aerosol transport modeling of dust, but the present study represents a first direct validation of the transport of IN-containing dust layers near the tropopause entering the North American continent.

[51] The ability of models such as STEM to predict encounters with dust plumes and the strong correspondence between dust concentrations and measured levels of IN in PACDEX and other recent programs suggest future promise for forecasting global IN fields for use in modeling dust impacts on clouds and precipitation.

[52] In regions where the dust was encountered outside of pollution plumes (e.g., Figure 4) the CCN concentrations (at 0.45% Sc) were generally low compared to regions where pollution was found (e.g., the lower part of the plume in Figure 2). Thus, outside of polluted regions dust does not appear to be a major factor in raising the total concentrations of CCN above maritime levels (at the supersaturations measured here), which suggests that a different situation exists in the North Pacific compared to the North Atlantic, based on the recent *Twohy et al.* [2009] results. More comparative studies of CCN from the two regions are planned. The Asian dust regions contain particles large enough to serve as giant CCN, even as they approach North America (Figure 4), if they are subsequently transported to lower altitudes where precipitation is formed. This may be more significant in terms of possible effects on North

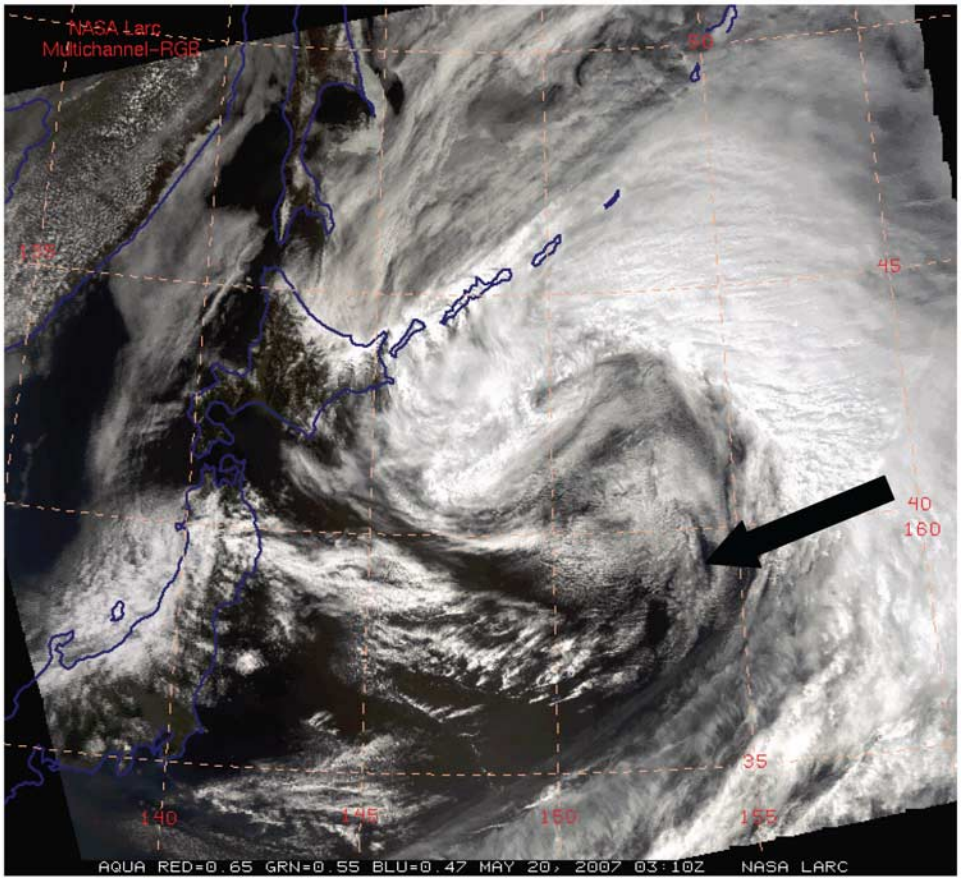

Figure 9. A visible image of the storm and the approximate location of the flight track (arrow) for the pass in Figure 8. Image courtesy of NASA Langley Research Center.

American precipitation than dust contributions to total CCN and is worthy of further study.

[53] Early examination of the encounters between pollution and Pacific springtime storms in PACDEX has to date produced only one occurrence where substantially enhanced droplet concentrations in polluted regions were noted. This occurred on the edges of a major Pacific extratropical cyclone. Thus, a widespread pollution effect on droplet concentrations in these storms seems unlikely, but this will be examined further in future studies.

[54] Significant concentrations of BC were observed both in the west and the east Pacific Ocean. These particles were observed through much of the troposphere, but were especially prevalent in the western Pacific below about 6 km altitude. A demarcation between higher concentrations of aerosols such as BC in the western Pacific and lower concentrations in the eastern Pacific was predicted by the STEM and generally confirmed by in situ vertical profiles during PACDEX.

[55] A major finding of the PACDEX project is that the percent of BC particles compared with the total number of accumulation mode particles increased significantly (by a factor of 2 to 4) with altitude, with peak values between 5 and 10 km. A similar observation was made in STEM when the STEM-predicted ratios of BC to sulfate aerosols were examined in the regions where the PACDEX observations were made at altitudes between 5 and 10 km. Thus, both the observations and model results suggest a maximum in the fraction of BC to accumulation mode/sulfate aerosols between 5 and 10 km. There are several factors that might explain these observations, including scavenging of more accumulation mode aerosols than BC at mid tropospheric altitudes. Sources of BC to the upper troposphere (e.g., from aircraft) or sources of accumulation mode particles to the lower troposphere might also produce such an effect. These will be investigated in future studies.

[56] **Acknowledgments.** NCAR is supported by the National Science Foundation (NSF). PACDEX was primarily supported by the NSF. P.J.D. and A.J.P. acknowledge support under NSF grant ATM-0611936. C.H.T. acknowledges support under NSF grant ATM-0612605. C.D.H. acknowledges support from the NSF under grants CHE503854 and ATM0613124. DMT participation in PACDEX was supported by NSF grant ATM-0612605. The authors thank Barry Huebert and Jorgen Jensen for helpful comments on the manuscript. Thanks are also due to the NCAR flight crew and the staff of NCAR's Earth Observing Laboratory for excellent support of the project.

References

Alexander, D. L. T., P. A. Crozier, and J. R. Anderson (2008), Brown carbon spheres in east Asian outflow and their direct radiative forcing properties, *Science*, *321*, 833–836, doi:10.1126/science.1155296.

Baumgardner, D., R. Subramanian, C. Twohy, J. Stith, and G. Kok (2008), Scavenging of black carbon by ice crystals over the northern Pacific, *Geophys. Res. Lett.*, *35*, L22815, doi:10.1029/2008GL035764.

Carmichael, G. R., et al. (2003), Regional-scale chemical transport modeling in support of intensive field experiments: Overview and analysis of the TRACE-P observations, *J. Geophys. Res.*, *108*(D21), 8823, doi:10.1029/2002JD003117.

DeMott, P. J., D. C. Rogers, S. M. Kreidenweis, Y. Chen, C. H. Twohy, D. Baumgardner, A. J. Heymsfield, and K. R. Chan (1998), The role of heterogeneous freezing nucleation in upper tropospheric clouds: Infer-

ences from SUCCESS, *Geophys. Res. Lett.*, *25*, 1387–1390, doi:10.1029/97GL03779.

DeMott, P. J., K. Sassen, M. R. Poellot, D. Baumgardner, D. C. Rogers, S. D. Brooks, A. J. Prenni, and S. M. Kreidenweis (2003), African dust aerosols as atmospheric ice nuclei, *Geophys. Res. Lett.*, *30*(14), 1732, doi:10.1029/2003GL017410.

Field, P. R., O. Mohler, P. Connolly, M. Kramer, R. Cotton, A. J. Heymsfield, H. Saathoff, and M. Schnaiter (2006), Some ice nucleation characteristics of Asian and Saharan desert dust, *Atmos. Chem. Phys.*, *6*, 2991–3006.

Georgii, H. W., and E. Kleinjung (1967), Relations between the chemical composition of atmospheric aerosol particles and the concentration of natural ice nuclei, *J. Rech. Atmos.*, *3*, 145–146.

Hadley, O. L., V. Ramanathan, G. R. Carmichael, Y. Tang, G. C. Roberts, and G. S. Mauger (2007), Trans-Pacific transport of black carbon and fine aerosols (D < 2.5 (μm) into North America, *J. Geophys. Res.*, *112*, D05309, doi:10.1029/2006JD007632.

Hirst, E., P. H. Kaye, R. S. Greenaway, P. Field, and D. W. Johnson (2001), Discrimination of micrometre-sized ice and super-cooled droplets in mixed-phase cloud, *Atmos. Environ.*, *35*, 33–47, doi:10.1016/S1352-2310(00)00377-0.

Huebert, B. J., T. Bates, P. B. Russell, G. Shi, Y. Kim, K. Kawamura, G. Carmichael, and T. Nakajima (2003), An overview of ACE-Asia: Strategies for quantifying the relationships between Asian aerosols and their climatic impacts, *J. Geophys. Res.*, *108*(D23), 8633, doi:10.1029/2003JD003550.

Husar, R. B., et al. (2001), Asian dust events of April 1998, *J. Geophys. Res.*, *106*(D16), 18,317–18,330, doi:10.1029/2000JD900788.

Jacob, D. J., J. H. Crawford, M. M. Kleb, V. S. Connors, R. J. Bendura, J. L. Raper, G. W. Sachse, J. C. Gille, L. Emmons, and C. L. Heald (2003), Transport and Chemical Evolution Over the Pacific (TRACE-P) aircraft mission: Design, execution, and first results, *J. Geophys. Res.*, *108*(D20), 9000, doi:10.1029/2002JD003276.

Jaffe, D., S. Tamura, and J. Harris (2005), Seasonal cycle and composition of background fine particles along the west coast of the US, *Atmos. Environ.*, *39*, 297–306, doi:10.1016/j.atmosenv.2004.09.016.

Kline, J., B. Huebert, S. Howell, B. Blomquist, J. Zhuang, T. Bertram, and J. Carrillo (2004), Aerosol composition and size versus altitude measured from the C-130 during ACE-Asia, *J. Geophys. Res.*, *109*, D19S08, doi:10.1029/2004JD004540.

Laursen, K. K., D. P. Jorgensen, G. P. Brasseur, S. L. Ustin, and J. R. Huning (2006), HIAPER: The next generation NSF/NCAR research aircraft, *Bull. Am. Meteorol. Soc.*, *87*, 896–909, doi:10.1175/BAMS-87-7-896.

Levin, Z., A. Teller, E. Ganor, and Y. Yin (2005), On the interactions of mineral dust, sea-salt particles, and clouds: A measurement and modeling study from the Mediterranean Israeli Dust Experiment campaign, *J. Geophys. Res.*, *110*, D20202, doi:10.1029/2005JD005810.

Mahowald, N., and L. M. Kiehl (2003), Mineral aerosol and cloud interactions, *Geophys. Res. Lett.*, *30*(9), 1475, doi:10.1029/2002GL016762.

Maring, H., D. L. Savoie, M. A. Izaguirre, L. Custals, and J. S. Reid (2003), Mineral dust aerosol size distribution change during atmospheric transport, *J. Geophys. Res.*, *108*(D19), 8592, doi:10.1029/2002JD002536.

Möhler, O., P. J. DeMott, G. Vali, and Z. Levin (2007), Microbiology and atmospheric processes: The role of biological particles in cloud physics, *Biogeosciences*, *4*, 1059–1071.

Noone, K. J., J. A. Ogren, J. Heintzenberg, R. J. Charlson, and D. S. Covert (1988), Design and calibration of a counterflow virtual impactor for sampling of atmospheric fog and cloud droplets, *Aerosol. Sci. Technol.*, *8*, 235–244, doi:10.1080/02786828808959186.

Pilewskie, P., J. Pommier, R. Bergstrom, W. Gore, S. Howard, M. Rabbette, B. Schmid, P. V. Hobbs, and S. C. Tsay (2003), Solar spectral radiative forcing during the Southern African Regional Science Initiative, *J. Geophys. Res.*, *108*(D13), 8486, doi:10.1029/2002JD002411.

Prenni, A. J., J. Y. Harrington, M. Tjernström, P. J. DeMott, A. Avramov, C. N. Long, S. M. Kreidenweis, P. Q. Olsson, and J. Verlinde (2007), Can ice nucleating aerosols affect Arctic seasonal climate? Bull, *Am. Meteorol. Soc.*, *88*(4), 541–550, doi:10.1175/BAMS-88-4-541.

Proffitt, M. H., and R. J. McLaughlin (1983), Fast-response dual beam UV-absorption ozone photometer suitable for use on stratospheric balloons, *Rev. Sci. Instrum.*, *54*, 1719–1728, doi:10.1063/1.1137316.

Pruppacher, H., and J. D. Klett (1997), *Microphysics of Clouds and Precipitation*, 954 pp., Springer, New York.

Ramanathan, V., et al. (2001), The Indian Ocean Experiment: An integrated assessment of the climate forcing and effects of the great Indo-Asian haze, *J. Geophys. Res.*, *106*(D22), 28,371–28,399, doi:10.1029/2001JD900133.

Richardson, M. S., et al. (2007), Measurements of heterogeneous ice nuclei in the western United States in springtime and their relation to aerosol characteristics, *J. Geophys. Res.*, *112*, D02209, doi:10.1029/2006JD007500.

Roberts, G., and A. Nenes (2005), A continuous-flow streamwise thermal-gradient CCN chamber for airborne measurements, *Aerosol. Sci. Technol.*, *39*, 206–221, doi:10.1080/027868290913988.

Rogers, D. C. (1988), Development of a continuous flow thermal gradient diffusion chamber for ice nucleation studies, *Atmos. Res.*, *22*, 149–181, doi:10.1016/0169-8095(88)90005-1.

Rogers, D. C., P. J. DeMott, S. M. Kreidenweis, and Y. Chen (2001), A continuous-flow diffusion chamber for airborne measurements of ice nuclei, *J. Atmos. Oceanic Technol.*, *18*, 725–741, doi:10.1175/1520-0426(2001)018<0725:ACFDCF>2.0.CO;2.

Rogers, R. R., and M. K. Yau (1989), *A Short Course in Cloud Physics*, 293 pp., Elsevier, New York.

Sassen, K. (2002), Indirect climate forcing over the western US from Asian dust storms, *Geophys. Res. Lett.*, *29*(10), 1465, doi:10.1029/2001GL014051.

Sassen, K., P. J. DeMott, J. M. Prospero, and M. R. Poellot (2003), Saharan dust storms and indirect aerosol effects on clouds: CRYSTAL-FACE results, *Geophys. Res. Lett.*, *30*(12), 1633, doi:10.1029/2003GL017371.

Schwarz, J. P., et al. (2006), Single-particle measurements of midlatitude black carbon and light-scattering aerosols from the boundary layer to the lower stratosphere, *J. Geophys. Res.*, *111*, D16207, doi:10.1029/2006JD007076.

Seinfeld, J. H., et al. (2004), ACE-ASIA—Regional climatic and atmospheric chemical effects of Asian dust and pollution, *Bull. Am. Meteorol. Soc.*, *85*(3), 367–380, doi:10.1175/BAMS-85-3-367.

Stohl, A., S. Eckhardt, C. Forster, P. James, and N. Spichtinger (2002), On the pathways and timescales of intercontinental air pollution transport, *J. Geophys. Res.*, *107*(D23), 4684, doi:10.1029/2001JD001396.

Twohy, C. H., A. J. Schanot, and W. A. Cooper (1997), Measurement of condensed water content in liquid and ice clouds using an airborne counterflow virtual impactor, *J. Atmos. Oceanic Technol.*, *14*, 197–202, doi:10.1175/1520-0426(1997)014<0197:MOCWCI>2.0.CO;2.

Twohy, C. H., et al. (2009), Saharan dust particles nucleate droplets in eastern Atlantic clouds, *Geophys. Res. Lett.*, *36*, L01807, doi:10.1029/2008GL035846.

VanCuren, R., and T. Cahill (2002), Asian aerosols in North America: Frequency and concentration of fine dust, *J. Geophys. Res.*, *107*(D24), 4804, doi:10.1029/2002JD002204.

van den Heever, S. C., G. Carrio, W. Cotton, P. DeMott, and A. Prenni (2006), Impacts of nucleating aerosol on Florida storms. part I: Mesoscale simulations, *J. Atmos. Sci.*, *63*, 1752–1775, doi:10.1175/JAS3713.1.

Yu, H., L. A. Remer, M. Chin, H. Bian, R. G. Kleidman, and T. Diehl (2008), A satellite-based assessment of transpacific transport of pollution aerosol, *J. Geophys. Res.*, *113*, D14S12, doi:10.1029/2007JD009349.

Zhang, R., G. Li, J. Fan, D. L. Wu, and M. J. Molina (2007), Intensification of Pacific storm track linked to Asian pollution, *Proc. Natl. Acad. Sci. U. S. A.*, *104*, 5295–5299, doi:10.1073/pnas.0700618104.

Zhu, A., V. Ramanathan, F. Li, and D. Kim (2007), Dust plumes over the Pacific, Indian, and Atlantic oceans: Climatology and radiative impact, *J. Geophys. Res.*, *112*, D16208, doi:10.1029/2007JD008427.

B. Adhikary, Center for Global and Regional Environmental Research, University of Iowa, 407 IATL/CGRER, Iowa City, IA 52242, USA.

J. Anderson, Mechanical and Aerospace Engineering, Arizona State University, Mail Code 6106, Tempe, AZ 85287, USA.

D. Baumgardner, Centro de Ciencias de la Atmósfera, Universidad Nacional Autónoma de México, Circuito Exterior s/n, Ciudad Universitaria, 04510 México City, Mexico.

T. Campos, W. A. Cooper, D. C. Rogers, and J. L. Stith, Earth Observing Laboratory, National Center for Atmospheric Research, Box 3000, Boulder, CO 80307, USA. (stith@ucar.edu)

G. Carmichael, Center for Global and Regional Environmental Research, University of Iowa, Iowa City, IA 52242, USA.

P. J. DeMott and A. J. Prenni, Department of Atmospheric Science, Colorado State University, 1371 Campus Delivery, Fort Collins, CO 80523, USA.

Y. Feng and V. Ramanathan, Center for Clouds, Chemistry and Climate, Scripps Institution of Oceanography, University of California, San Diego, 9500 Gilman Drive, MC 0221, La Jolla, CA 92093-0221, USA.

R. Gao, Chemical Sciences Division, NOAA Earth System Research Laboratory, 325 Broadway R/CSD 6, Boulder, CO 80305, USA.

C. D. Hatch, Department of Chemistry, Hendrix College, 1600 Washington Avenue, Conway, AR 72032, USA.

G. C. Roberts, Climate, Atmospheric Science and Physical Oceanography, Scripps Institution of Oceanography, University of California, San Diego, 9500 Gilman Drive, MC 0221, La Jolla, CA 92093-0221, USA.

C. H. Twohy, College of Oceanic and Atmospheric Sciences, Oregon State University, 104 COAS Administration Building, Corvallis, OR 97331, USA.